Research Article

Experimental and numerical investigation of T section connections

Mahmut Kılıç [a,*] , Abdulkadir Cüneyt Aydın [a] , Merve Sağıroğlu [b] , Mahyar Maali [b]

[a] *Department of Civil Engineering, Atatürk University, 25240 Erzurum, Turkey*
[b] *Department of Civil Engineering, Erzurum Technical University, 25050 Erzurum, Turkey*

ABSTRACT

The paper summarizes recent experimental research on determining the full-range behaviour of steel beam-to-column connections. Unlike the connection types in the literature, numerical modeling was done with various experiments to determine the behavior of two types of connection types. In these joints, T joints have been studied, but unlike the literature, T joint's element is made of plates; It was obtained from 1/2 IPE profile, not by welding. Thus, it is thought that the problems such as workmanship errors, break point formation and in situ welding failures, which occur in the welding of T joints, are eliminated. Necessary studies have been carried out to have sufficient information about the behavior of the T joint to be manufactured from the IPE profile and thus to provide the opportunity for its use. In the light of the data obtained, numerical modeling is done and the torque rotation relation and behavior of semi-rigid joints are numerically modeled. Thus, thanks to the calibrated model with the experiments, the closest results to the real behavior were obtained for the unexamined combinations.

1. Introduction

Beam-column joints play an important role in the behavior of frame systems. For more than half a century beam-column behavior has been studied both experimentally and theoretically. In calculation methods used in steel structures, beam column joints are considered to be hinged or rigid. According to these theories, there is no local rotation in the elements in rigid joints, and when a moment is influenced from outside, this moment is distributed in proportion to the rigidity of the elements. However, in reality, the joints are neither fully rigid nor fully articulated. In experimental studies conducted in recent years, it has been observed that more accurate results are obtained by accepting combinations as semi-rigid.

The bolted beam-to-column connections are an important part of steel frames. It is a significant issue to design beam-to-column connection of steel building's frames because the behavior of beam-to-column connection significantly influences the performance of the whole frame. Different connections types have been suggested

and developed. Its bolted connections are usually applied to connect the beam to the column using some joint elements such as T-stubs, end-plates, and steel angles. Various parameters such as loading condition, connection details, and materials, affect the connection characteristics. The loading condition tests (Coelho and Bijlaard, 2007), and numerical analyses (Tagawa and Gurel, 2005; Kukreti and Zhou, 2006; Shi et al., 2008, Díaz et al., 2011) were carried out to evaluate the beam-to-column bolted connection. On the other hand, the stiffening of connections improve the performance of structures. The bolted connections of the beam-to-columns are usually designed by engineers as semi-rigid. (Tagawa and Liu, 2014; Tagawa et al., 2020).

The T-stub connections were experimentally investigated to the effect of beam-to-columns connection behavior. Its bolted connections often behave as semi-rigid connections so that their modeling requires many issues to be faced. Regarding the ability of beam-to-column joints in providing adequate plastic rotation supply and energy dissipation capacity for seismic design applications. A suitable joint semi-rigid design can lead to a plas-

tic rotation supply compatible with the plastic rotation demand under seismic motion (Piluso and Rizzano, 2008). The information about the behavior of the joints achieved by experiments in order to understand the behavior of steel structures. However, different ways such as analytical, empirical, mechanical, numerical can be defined as the combination behavior (Batho and Rowan, 1934; Abdalla and Chen, 1995). The first application of bolts in steel structures had been started in 1950s, which was about the geometric and mechanical properties of rigid joints. From the 1950s to the present, different types have been investigated by researchers such as type of junction, upper and lower hull body type double-junction type, double-frame body joint type, single-frame body joint type, forehead plate joint type, beam-joint combination types. By comparing the results obtained from the models with the experimental data, it was stated that with the finite-element model, time and cost savings as well as the visual preparation of force and stress distributions to understand the behavior of the combination provided great advantages.

In recent years, many studies have been done on the analysis and design of space steel frames. In this research, they have developed a program for analyzing and designing space steel frames (Aydın et al., 2015a).

With stiffener and without stiffener, moment-rotation behavior was compared to the EN1993-1-8 specification (Aydın et al., 2015b).

The ductility of a joint (Ψ_j) is a property that reflects the length of the yield plateau of the moment-rotation response. The proposed definition of the ductility of a joint is the difference between the rotation value corresponding to the joint plastic resistance, $\theta_{M.Rd}$, and the total rotation capacity, θ_{Cd} (Aydın et al., 2015a, 2015b) (Fig. 2). Thus, the ductility of a joint relates the maximum rotation of the joint, θ_{Cd}, to the rotation value corresponding to the joint's plastic flexural resistance, $\theta_{M.Rd}$ (Maali et al., 2016, 2017, 2018a, 2018b).

2. Experimental Program

2.1. Test details

18 experiments were summarised in Table 1. In this study, T connections were obtained by 83 cuttings from standard IPE profiles, and a seat angle stiffener was selected. Fig. 1 shows the test details. Angle T connections were studied, but unlike the literature, not by welding, but by the 1/2 IPE profile. Thus, it is thought that problems such as workmanship errors that occur in the sources of T-connections, break-point formation, inadequate performance of on-site welding has been removed. T connections obtained from IPE profiles were experimented with using 1 and 2 rows of bolts. Thus, the effect of the row and number of bolts in the T profile body on the moment-rotation behavior was investigated.

In this research, each group compared with each other and other groups. The beam profile is from the IPE240 profile. The bolts are used in M8.8 quality and 14mm diameter, and finally the lower bracket L60*6 and 120mm width. Columns HEB160 is selected as standard.
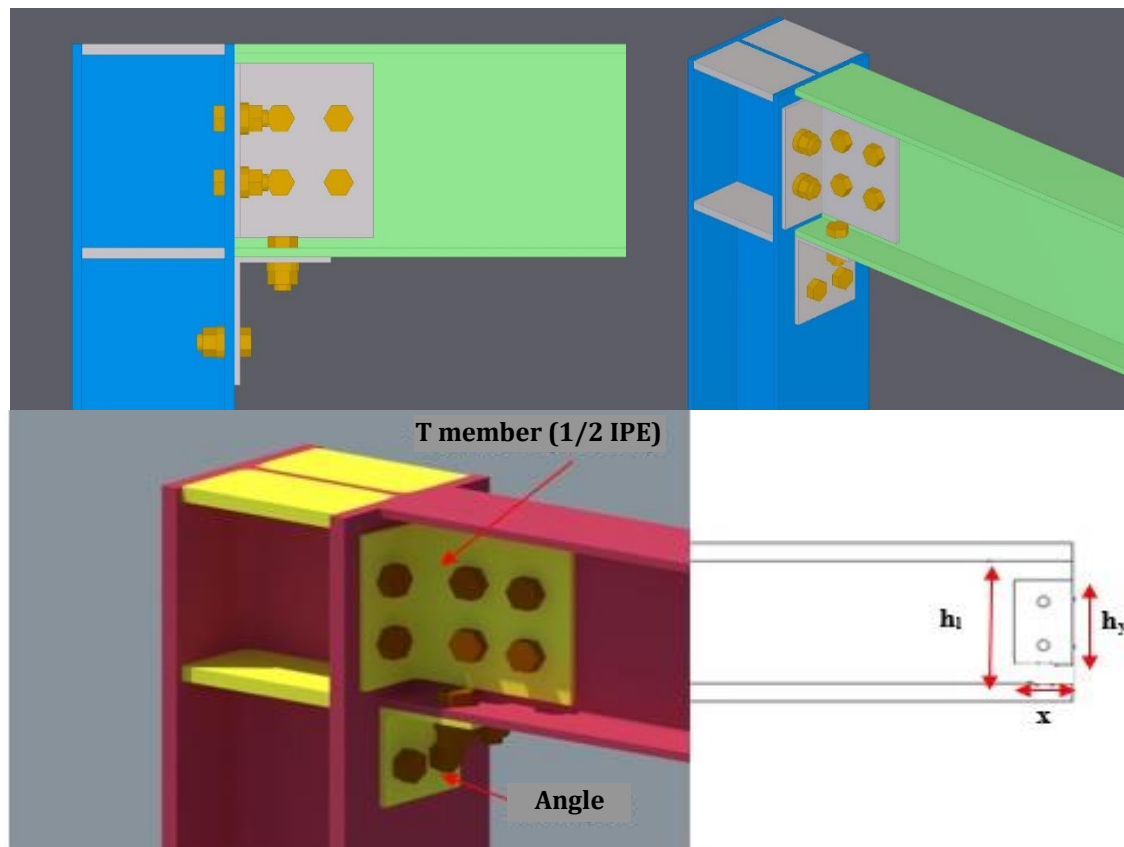

Fig. 1. Seat angle T connections.

Table 1. The geometry of the test.

Group	Specimen	$H_{max}=$ $h_{y\,max}/h_1$	$H_{min}=$ $h_{y\,min}/h_1$	$H_{mid}=$ $h_{y\,med}/h_1$	X_{max} (mm)	X_{min} (mm)	½ T profile	Number of bolts
Angle T300	B240-T300-H_{max}-X_{max}-2-14-L60 (1)	1=22			215		IPE 300	2
	B240-T300-H_{min}-X_{max}-2-14-L60 (2)		0.63=14		215		IPE 300	2
	B240-T300-H_{mid}-X_{max}-2-14-L60 (3)			0.82=18	215		IPE 300	2
	B240-T300-H_{max}-X_{min}-1-14-L60 (4)	1=22				89	IPE 300	1
	B240-T300-H_{min}-X_{min}-1-14-L60 (5)		0.63=14			89	IPE 300	1
	B240-T300-H_{mid}-X_{min}-1-14-L60 (6)			0.82=18		89	IPE 300	1
Angle T270	B240-T270-H_{max}-X_{max}-2-14-L60 (7)	1=22			215		IPE 270	2
	B240-T270-H_{min}-X_{max}-2-14-L60 (8)		0.63=14		215		IPE270	2
	B240-T270-H_{mid}-X_{max}-2-14-L60 (9)			0.82=18	215		IPE 270	2
	B240-T270-H_{max}-X_{min}-1-14-L60 (10)	1=22				89	IPE 270	1
	B240-T270-H_{min}-X_{min}-1-14-L60 (11)		0.63=14			89	IPE270	1
	B240-T270-H_{mid}-X_{min}-1-14-L60 (12)			0.82=18		89	IPE270	1
Angle T240	B240-T240-H_{max}-X_{max}-2-14-L60 (13)	1=22			215		IPE240	2
	B240-T240-H_{min}-X_{max}-2-14-L60 (14)		0.63=14		215		IPE240	2
	B240-T240-H_{mid}-X_{max}-2-14-L60 (15)			0.82=18	215		IPE240	2
	B240-T240-H_{max}-X_{min}-1-14-L60 (16)	1=22				89	IPE240	1
	B240-T240-H_{min}-X_{min}-1-14-L60 (17)		0.63=14			89	IPE240	1
	B240-T240-H_{mid}-X_{min}-1-14-L60 (18)			0.82=18		89	IPE240	1

In the study, S235 steel grade, which is more common in the market, was preferred for all test samples. To observe the actual combined behaviour experimentally, the beam dimensions were chosen as 1500 mm. The specimens were subjected to a static force applied by a 900 kN hydraulic jack with a maximum piston stroke of 300 mm. Tests were performed under displacement control with a constant speed of 0.01 mm/s up to the collapse of the specimens. To prevent the lateral torsional buckling of the beam while loading, a two-column guidance device near the beam was provided. Fig. 2 shows that test setup.

The primary requirements of the instrumentation were the measurement of: The applied load (P); the displacements (DT) of the connection, beam, and angle T connection, the strains at the angle T connections. The results were collected using a data logging device that recorded all measurements and the load cells at one-second intervals. All the data were recorded for the duration of the test. Displacements were measured using linear variable displacement transducers with a maximum displacement of 300 mm. Two strain gauges (St) of TML YEFLA- 5 (maximum strain of 15-20%) used for calculated strain. The locations of LVDTs are given in Table 2.
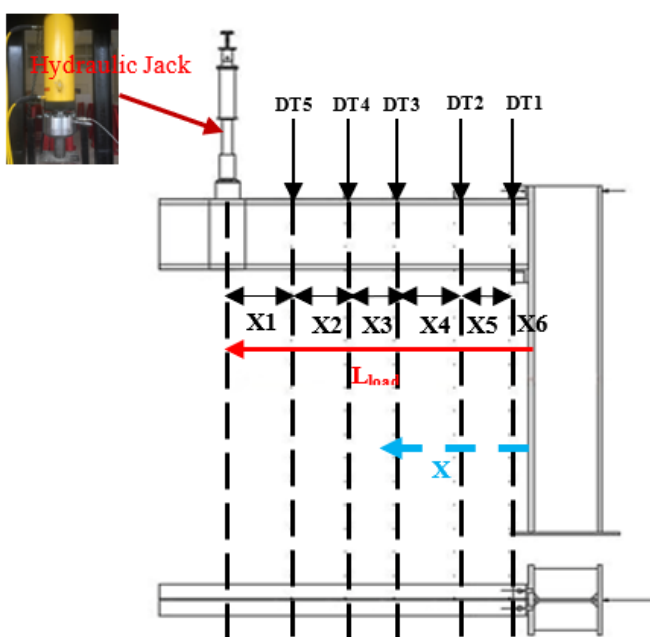

Fig. 2. Test setup.

Table 2. Locations of the displacement transducers (*DT* = LVDT).

Group	Specimen	X_1 (mm)	X_2 (mm)	X_3 (mm)	X_4 (mm)	X_5 (mm)	X_6 (mm)
Angle T300	B240-T300-H_{max}-X_{max}-2-14-L60 (1)	390	280	315	197	140	45
	B240-T300-H_{min}-X_{max}-2-14-L60 (2)	330	290	330	190	130	120
	B240-T300-H_{mid}-X_{max}-2-14-L60 (3)	330	295	320	200	130	90
	B240-T300-H_{max}-X_{min}-1-14-L60 (4)	280	320	270	200	145	115
	B240-T300-H_{min}-X_{min}-1-14-L60 (5)	255	328	293	190	160	130
	B240-T300-H_{mid}-X_{min}-1-14 -L60 (6)	305	332	285	195	155	88
Angle T270	B240-T270-H_{max}-X_{max}-2-14-L60 (7)	340	290	330	200	130	120
	B240-T270-H_{min}-X_{max}-2-14-L60 (8)	330	290	320	195	135	120
	B240-T270-H_{mid}-X_{max}-2-14-L60 (9)	335	295	320	190	135	100
	B240-T270-H_{max}-X_{min}-1-14-L60 (10)	320	330	175	110	335	110
	B240-T270-H_{min}-X_{min}-1-14-L60 (11)	290	335	300	205	130	14
	B240-T270-H_{mid}-X_{min}-1-14-L60 (12)	305	335	288	203	144	86
Angle T240	B240-T240-H_{max}-X_{max}-2-14-L60 (13)	390	290	320	193	13	45
	B240-T240-H_{min}-X_{max}-2-14-L60 (14)	320	285	325	195	135	130
	B240-T240-H_{mid}-X_{max}-2-14-L60 (15)	405	300	315	190	140	80
	B240-T240-H_{max}-X_{min}-1-14-L60 (16)	380	335	275	190	150	40
	B240-T240-H_{min}-X_{min}-1-14-L60 (17)	290	334	295	200	145	115
	B240-T240-H_{mid}-X_{min}-1-14-L60 (18)	298	325	294	203	140	100

2.2. Numerical models

The element types to be used in a combination to be analyzed in the ANSYS program should be defined beforehand. The staff in general; beam, plane, shell, solid and link (beam, plane, shell, solid and connection) elements are known for structural analysis. Models for this study are defined using solid elements. One of the most important steps in a finite-element analysis is the creation of the network structure. The ANSYS program has several mesh options available. In this study, the concentration of desired analyzes on the junction area, the regions where the stresses are intense and the junction area are kept smaller in the junction area and chosen larger in the girder and beam. The network structure can be seen in Fig. 3. Mesh sizing is important for accurate stress and displacement values. For this purpose, selected meshing type, the tetrahedron mesh divides various sizing meshes starting with 200 mm. When the stress and displacement values are stable, this mesh sizing can be applicable for FEM analysis.
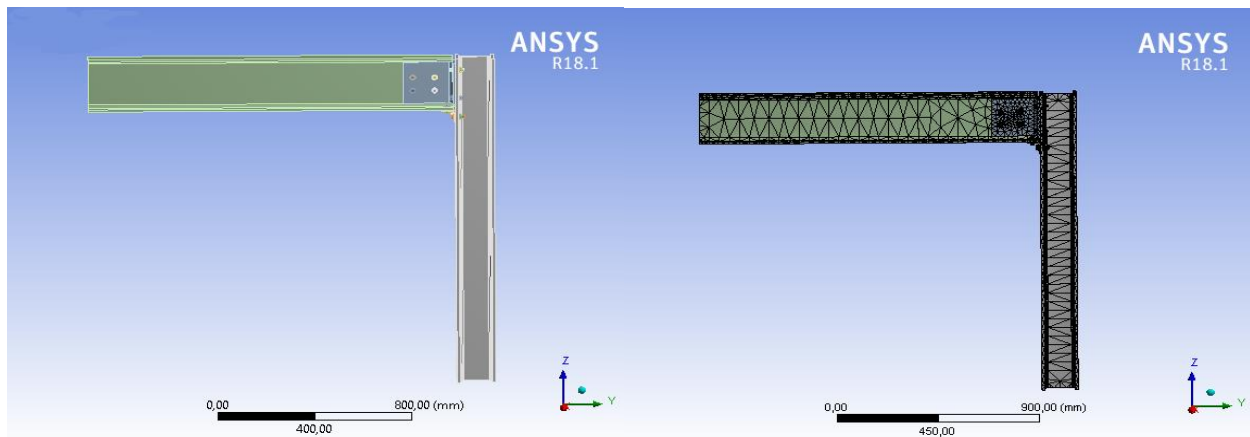
Fig. 3. Finite element modeling.

3. Experimental Results

In these experiments, experiments will be carried out by grouping as the width of the cornier (*X*), X_{max} containing 2 rows of bolts and X_{min} containing a single row of bolts. European and American Standards were taken into consideration while making this grouping selection. In these two groups, the *H* ratio, which we define as the ratio of corneal width h_y to beam trunk length h_1, is foreseen, and it is planned to make comparisons according to the *H* ratio in the experiment results. *H* values are divided into three groups as H_{max}, H_{mid} and H_{min}. Fig. 4 shows the major features of the moment rotation curve of Eurocode 3. The term "Knee-range" defined in Fig. 4 is the slope of the line drawn in the non-linear region of the moment-rotation curve.

3.1. T300, T270, T240 types double row bolted connection series

Fig. 5 shows the moment rotation curves of the T300, T270, and T240 angle groups. Fig. 6 shows that experiment models. Table 3 summarizes the experiment results.
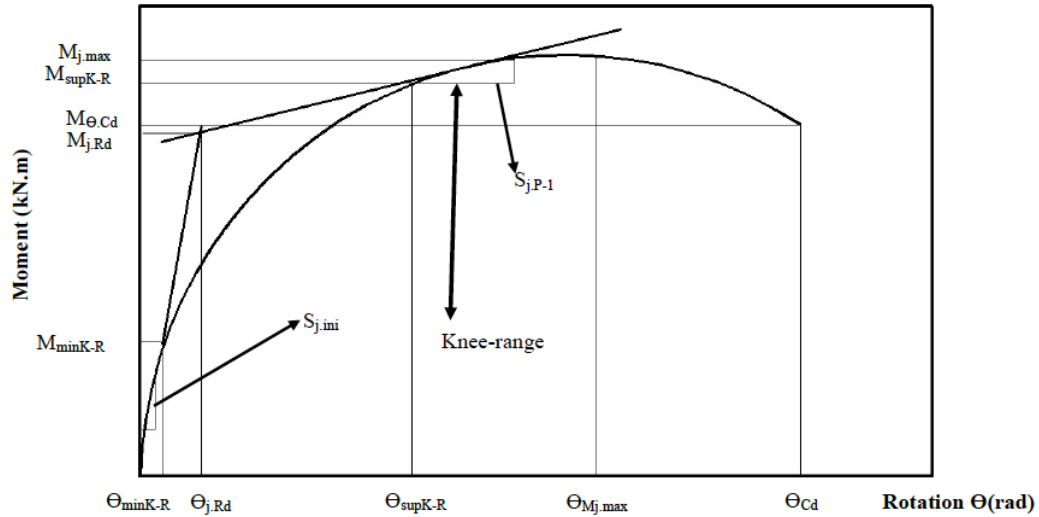
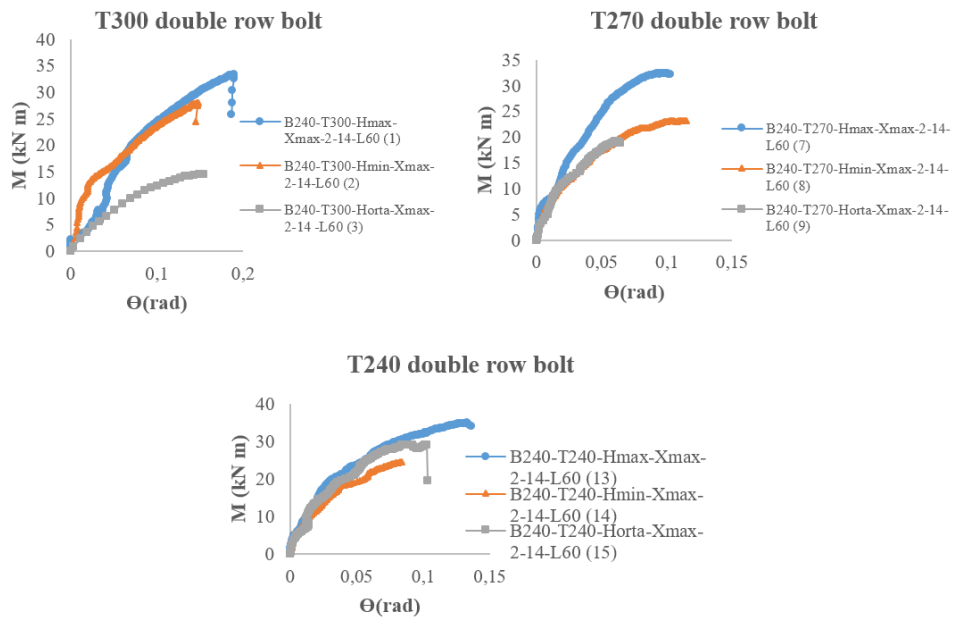**Fig. 4.** Moment–rotation curve characteristics.

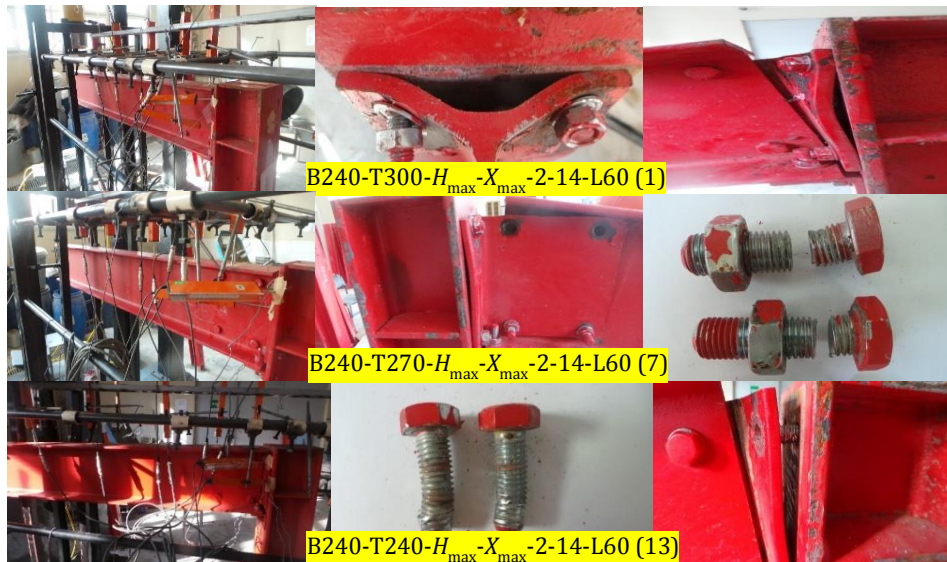**Fig. 5.** T300-270-240 group moment-rotation curves of double row bolt tests.

Fig. 6. Experiment models.

Table 3. Test results.

Experiment	Resistance (kN.m)				Stiffness (kN.m/rad)			Rotation (rad)					Ψ_j	$\Psi_{j.max\ load}$	Energy dissipated (kN.m.rad)
	KR (knee-range)	$M_{j.Rd}$	$M_{j.max}$	$M_{\theta Cd}$	$S_{j.ini}$	$S_{j.p-1}$	$S_{j.ini}/S_{j.p-1}$	$\theta_{M.Rd}$	$\theta_{min.KR}$	$\theta_{Msup.kR}$	$\theta_{Mj.max}$	θ_{Cd}			
B240-T300-H_{max}-X_{max}-2-14-L60 (1)	7.52-22.36	21.22	32.76	32.52	0.71	0.28	2.57	0.079	0.031	0.086	0.19	0.190	2.40	2.40	3.08
B240-T300-H_{min}-X_{max}-2-14-L60 (2)	10.13-19.16	13.88	27.95	27.48	2.33	0.29	7.88	0.018	0.014	0.067	0.15	0.150	8.33	8.33	2.06
B240-T300-H_{mid}-X_{max}-2-14 -L60 (3)	3.5-12-86	11.95	14.47	14.47	1.22	0.17	7.19	0.069	0.018	0.110	0.15	0.150	2.17	2.17	1.08
B240-T270-H_{max}-X_{max}-2-14-L60 (7)	6.79-29.57	19.73	23.16	23.16	2.52	0.07	33.51	0.03	0.0091	0.093	0.11	0.110	5.00	5.00	1.64
B240-T270-H_{min}-X_{max}-2-14-L60 (8)	6.63-22.57	19.73	23.16	23.16	2.52	0.07	33.51	0.03	0.0091	0.093	0.11	0.110	3.66	3.66	1.27
B240-T270-H_{mid}-X_{max}-2-14-L60 (9)	3.27-15.32	9.92	19.14	18.90	1.54	0.26	6.013	0.011	0.0031	0.040	0.062	0.064	5.82	5.82	0.60
B240-T240-H_{max}-X_{max}-2-14-L60 (13)	5.91-27.40	22.71	34.85	33.98	1.64	0.22	7.43	0.029	0.0057	0.065	0.13	0.140	4.83	4.48	2.38
B240-T240-H_{min}-X_{max}-2-14-L60 (14)	4.22-20.79	13.77	24.5	24.42	1.90	0.21	8.91	0.012	0.0034	0.058	0.08	0.083	6.92	6.66	1.01
B240-T240-H_{mid}-X_{max}-2-14-L60 (15)	7.37-27.03	23.01	28.93	28.93	1.80	0.15	12.26	0.024	0.0064	0.068	0.102	0.102	4.25	4.25	1.47

The plastic flexural resistance, $M_{j.Rd}$, which corresponds to the intersection point of the revious two regression lines obtained for the initial stiffness ($S_{j.ini}$) and for the post-limit stiffness ($S_{j.p-l}$) and its corresponding rotation $\theta_{M.Rd}$;

The maximum bending moment, $M_{j.max}$, and its corresponding rotation, $\theta_{M.j.max}$;

The knee-range of the $M–\theta$ curve, which is defined as the transition zone between the initial and post-limit stiffness, with its lower boundary at $M_{min.k-R}$ and rotation $\theta_{min.k-R}$, and with its upper limit at $M_{sup.k-R}$ and rotation $\theta_{sup.k-R}$;

The bending moment capacity, $M_{\theta.Cd}$, and its corresponding rotation capacity, θ_{cd}.

The ductility of a joint (Ψ_j) is a property that reflects the length of the yield plateau of the moment-rotation response. The proposed definition of the ductility of a joint is the difference between the rotation value corresponding to the joint plastic resistance, $\theta_{M.Rd}$, and the total rotation capacity, θ_{Cd}, Thus, the ductility of a joint relates the maximum rotation of the joint, θ_{Cd}, to the rotation value corresponding to the joint's plastic flexural resistance, $\theta_{M.Rd}$.

Comparisons of T300, T270 and T240 type connection combinations in their own groups are summarized in Table 4.

Moment-strain graphics of the experiments are shown in Figure 7.

Table 5 shows the comparison of T300, T270, T240 Double row bolted connections according to H_{max}, H_{min}, H_{mid} state.

Table 4. Comparison of T300, T270, T240 double row bolted joints in their own groups.

Exp.	Resistance (kN.m)			Stiffness (kN.m/rad)			Rotation (rad)					Ψ_j	$\Psi_{j.max\ load}$	Energy dissipated (kN.m.rad)
	$M_{j.Rd}$	$M_{j.max}$	$M_{\theta Cd}$	$S_{j.ini}$	$S_{j.p-1}$	$S_{j.ini}/S_{j.p-1}$	$\theta_{M.Rd}$	$\theta_{min.KR}$	$\theta_{Msup.kR}$	$\theta_{Mj.max}$	θ_{Cd}			
1--2	34.590	14.683	15.498	-228.169	-3.571	-206.615	77.215	54.839	22.093	21.053	21.053	-247.083	-247.083	33.117
1--3	43.685	55.830	55.504	-71.831	39.286	-179.767	12.658	41.935	-27.907	21.053	21.053	9.583	9.583	64.935
2--3	13.905	48.229	47.344	47.639	41.379	8.756	-283.333	-28.571	-64.179	0.000	0.000	73.950	73.950	47.573
7--8	0.000	0.000	0.000	0.000	0.000	0.000	0.000	0.000	0.000	0.000	0.000	26.800	26.800	22.561
7--9	49.721	17.358	18.394	38.889	-271.429	82.056	63.333	65.934	56.989	43.636	41.818	-16.400	-16.400	63.415
8--9	49.721	17.358	18.394	38.889	-271.429	82.056	63.333	65.934	56.989	43.636	41.818	-59.016	-59.016	52.756
13--14	39.366	29.699	28.134	-15.854	4.545	-19.919	58.621	40.351	10.769	38.462	40.714	-43.271	-48.661	57.563
13--15	-1.321	16.987	14.862	-9.756	31.818	-65.007	17.241	-12.281	-4.615	21.538	27.143	12.008	5.134	38.235
14--15	-67.102	-18.082	-18.468	5.263	28.571	-37.598	-100.000	-88.235	-17.241	-27.500	-22.892	38.584	36.186	-45.545

Table 5. Comparison of T300, T270, T240 double row bolted connections according to H_{max}, H_{min}, H_{mid} state.

Exp.	Resistance (kN.m)			Stiffness (kN.m/rad)			Rotation (rad)					Ψ_j	$\Psi_{j.max\ load}$	Energy dissipated (kN.m.rad)
	$M_{j.Rd}$	$M_{j.max}$	$M_{\theta Cd}$	$S_{j.ini}$	$S_{j.p-1}$	$S_{j.ini}/S_{j.p-1}$	$\theta_{M.Rd}$	$\theta_{min.KR}$	$\theta_{Msup.kR}$	$\theta_{Mj.max}$	θ_{Cd}			
1--7	7.022	29.304	28.782	-254.930	75.000	-1203.891	62.025	70.645	-8.140	42.105	42.105	-108.333	-108.333	46.753
1--13	-7.022	-6.380	-4.490	-130.986	21.429	-189.105	63.291	81.613	24.419	31.579	26.316	-101.250	-86.667	22.727
7--13	-15.104	-50.475	-46.718	34.921	-214.286	77.828	3.333	37.363	30.108	-18.182	-27.273	3.400	10.400	-45.122
2--8	-42.147	17.138	15.721	-8.155	75.862	-325.254	-66.667	35.000	-38.806	26.667	26.667	56.062	56.062	38.350
2--14	0.793	12.343	11.135	18.455	27.586	-13.071	33.333	75.714	13.433	46.667	44.667	16.927	20.048	50.971
8--14	30.208	-5.786	-5.440	24.603	-200.000	73.411	60.000	62.637	37.634	27.273	24.545	-89.071	-81.967	20.472
3--9	16.987	-32.274	-30.615	-26.230	-52.941	16.370	84.058	82.778	63.636	58.667	57.333	-168.203	-168.203	44.444
3--15	-92.552	-99.931	-99.931	-47.541	11.765	-70.515	65.217	64.444	38.182	32.000	32.000	-95.853	-95.853	-36.111
9--15	-131.956	-51.149	-53.069	-16.883	42.308	-103.892	-118.182	-106.452	-70.000	-64.516	-59.375	26.976	26.976	-145.000

B240-T300-H$_{orta}$-X$_{max}$-2-14 -L60 (3)

B240-T270-H$_{orta}$-X$_{max}$-2-14-L60 (9)

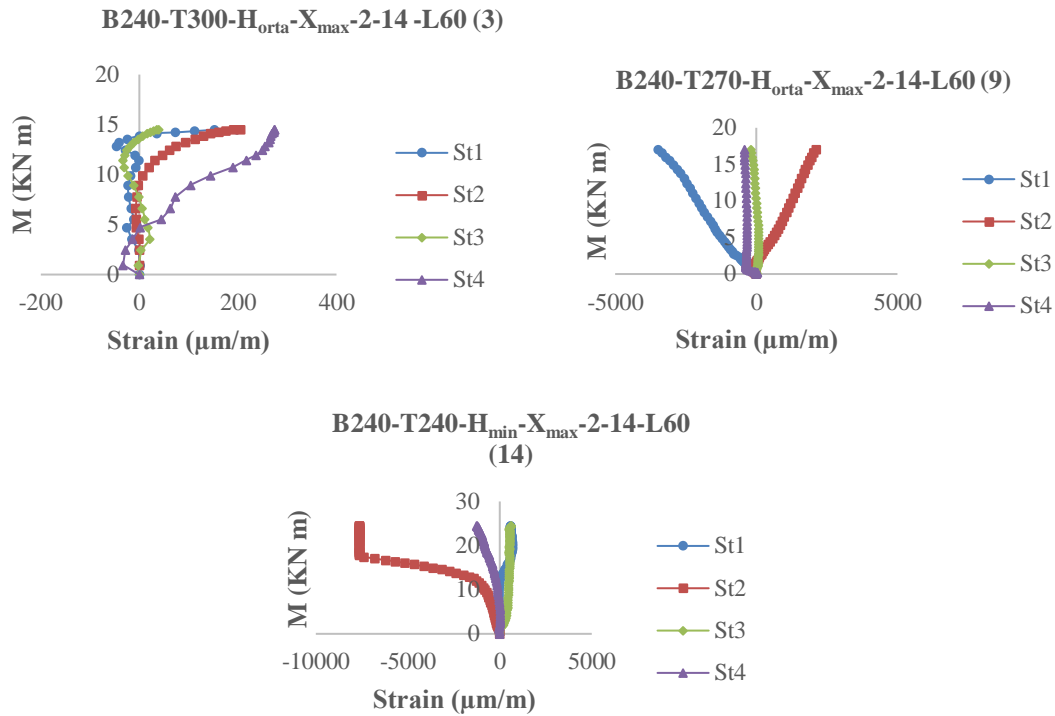**B240-T240-H$_{min}$-X$_{max}$-2-14-L60 (14)**

Fig. 7. Moment–strain curves for T300-T270 and T240 type double row bolts.

3.1.1. Failure mechanism

According to Eurocode 3, three types of breaking performance have been proposed for face plate joints. The first kind of breakage is that there is only deformation in the plate (Fig. 8a). The second kind of breakage is deformation and bolt breakage (Fig. 8b), and the third type is just bolt breakage (Fig. 8c). As seen in Fig. 8, this kind of cutting and breaking is the first kind of breaking situation. In other words, in the proposed combination, the first kind of breakage occurs.

It is observed that $M_{j.Rd}$, $M_{j.max}$ and $M_{\theta cd}$ value increased in all groups with the increase of H value. Looking at the $M_{j.Rd}$, $M_{j.max}$ and $M_{\theta cd}$ values; it is seen that the highest value in the T300 and T270 group is in the H_{max}-X_{max} group and the T240 group it is also in H_{max}-X_{max} and H_{mid}-X_{max}. Looking at the T300 and T270 groups, it is seen that H_{mid} values are smaller than H_{min} values. That is, as the thickness (t) of the joint increases, H_{max} joint types should be selected. Considering the combinations of H_{min} and H_{mid}, H_{min} should be chosen since it is economically more convenient. As the H value increases, $M_{j.Rd}$, $M_{j.max}$ and $M_{\theta cd}$ value increase.

B240-T300-*H*$_{mid}$-*X*$_{max}$-2-14 -L60 (3)

B240-T240 *H*$_{min}$-*X*$_{max}$-2-14-L60 (14)

B240-T270-*H*$_{min}$-*X*$_{max}$-2-14-L60 (8)

Fig. 8. Collapse models.

The highest $M_{j.Rd}$ change was seen as an increase of 49.72% when the H_{max}-X_{max} and H_{mid}-X_{max} groups were compared in the T270 group.

The highest $M_{j.max}$ change was observed in the H_{max}-X_{max} group in the T300 group and a 55.50% increase in the H_{mid}-X_{max} group.

The highest $M_{\theta Cd}$ change was observed in the H_{max}-X_{max} group in the T300 group and a 55.50% increase in the H_{mid}-X_{max} group.

As the thickness of the T joint element increases, the stiffness decreases. H_{mid} values were found to be the largest. So they are the most rigid connections.

$\theta_{M.Rd}$ value increases as T combination thickness and H increase. The highest variation was seen in the H_{max}-X_{max} and H_{min}-X_{max} groups of the T300 group, with an increase of 77.21%.

$\theta_{Mj.max}$ value increases as the T connection's thickness increases. The highest change was in the H_{max}-X_{max} and H_{mid}-X_{max} group in the T270 group, at +43.63%.

The θ_{Cd} value varies depending on the H value. This change is directly proportional. As the T connection's thickness increases, θ_{Cd} value increases. The highest change was in the H_{max}-X_{max} and H_{mid}-X_{max} group in the T270 group, at +41.81%.

The BB value decreased as the thickness increased. H_{min} values were found to be higher than H_{max} and H_{mid} values. If we want the Ψ_j values to be high, it is recommended to use H_{min}.

It is seen that $\Psi_{j.max load}$ value decreases with increasing thickness. It was observed that H_{min} value was higher than H_{max} and H_{mid} value. If we want the CC values to be too high, it is recommended to use H_{min} profile.

As the thickness increased, an increase in energy dissipated values was observed. When each group is evaluated within itself, energy dissipated increased as H increased. The best results are achieved when the wall thickness is high, and the H value is maximum.

3.1.2. Finite element models

The model pictures of finite elements for experiments using T300, T270 and T240 double row bolts are shown in Fig. 9. The results obtained from the curves are given in Table 6. Comparison of finite elements with experimental results is given in Table 7.
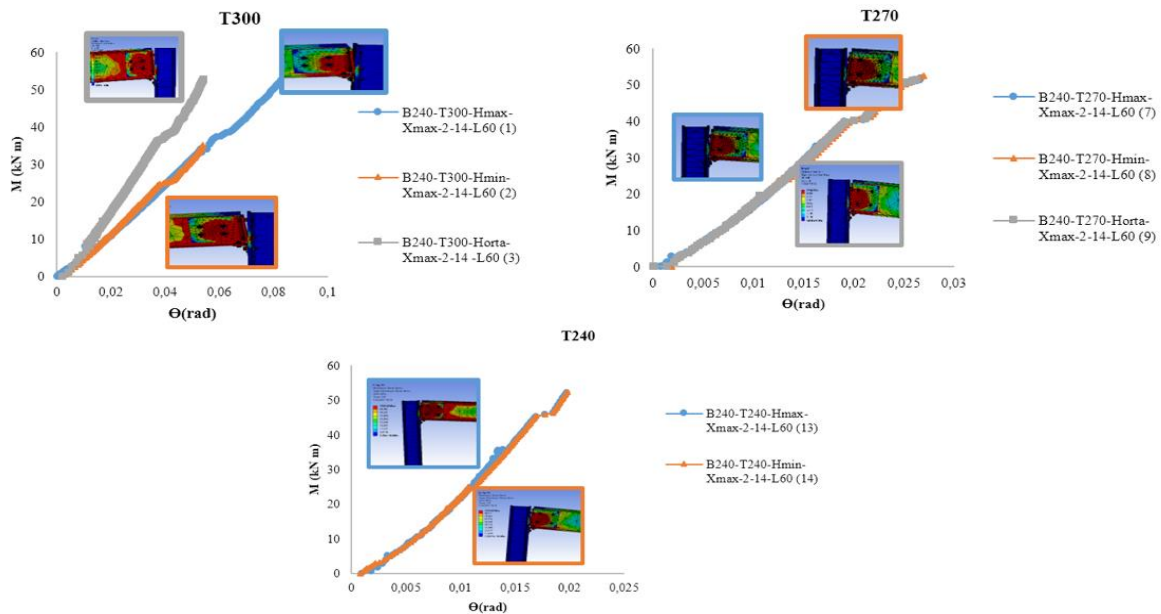

Fig. 9. T300-270-240 group moment-rotation curves of double row bolt finite element models.

Table 6. Model results of T300, T270, T240 double row bolt finite element models.

Experiment	Resistance (kN.m)			Stiffness (kN.m/rad)			Rotation (rad)					Ψ_j	$\Psi_{j.max load}$	Energy dissipated (kN.m.rad)
	KR (knee-range)	$M_{j.Rd}$	$M_{j.max}$	$M_{\theta Cd}$	$S_{j.ini}$	$S_{j.p-1}$	$S_{j.ini}/S_{j.p-1}$	$\theta_{M.Rd}$	$\theta_{min.KR}$	$\theta_{Msup.kR}$	$\theta_{Mj.max}$	θ_{Cd}			
B240-T300-H_{max}-X_{max}-2-14-L60 (1)	36.72-38.75	37.85	52.45	52.45	1.07	1.40	0.764	0.041	0.039	0.043	0.083	0.083	2.024	2.024	2.1767
B240-T300-H_{min}-X_{max}-2-14-L60 (2)	24.80-25.40	24.95	35.01	35.01	0.88	0.66	1.333	0.039	0.039	0.041	0.053	0.053	1.359	1.359	0.9278
B240-T300-H_{mid}-X_{max}-2-14 -L60 (3)	37.20-38.29	37.50	54.69	52.69	0.77	0.70	1.100	0.061	0.058	0.063	0.054	0.054	0.885	0.885	1.4226
B240-T270-H_{max}-X_{max}-2-14-L60 (7)	39.05-47.64	40.51	51.85	51.85	0.92	0.49	1.878	0.021	0.019	0.023	0.026	0.026	1.238	1.238	0.6741
B240-T270-H_{min}-X_{max}-2-14-L60 (8)	22.50-29.75	23.63	52.50	52.50	0.92	0.77	1.195	0.014	0.013	0.015	0.026	0.026	1.857	1.857	0.6825
B240-T270-H_{mid}-X_{max}-2-14-L60 (9)	39.15-47.54	40.50	51.40	51.40	0.92	0.49	1.878	0.021	0.018	0.021	0.025	0.025	1.190	1.190	0.6425
B240-T240-H_{max}-X_{max}-2-14-L60 (13)	34.24-35.76	34.70	52.09	52.09	0.99	0.74	1.338	0.014	0.0139	0.0143	0.019	0.019	1.357	1.357	0.4949
B240-T240-H_{min}-X_{max}-2-14-L60 (14)	45.33-46.84	46.33	52.38	52.38	0.79	0.73	1.082	0.0179	0.017	0.018	0.019	0.019	1.061	1.061	0.4976

Table 7. T300, T270, T240 type double-row finite element model and comparison of experimental results.

Exp.	Resistance (kN.m)			Stiffness (kN.m/rad)			Rotation (rad)					Ψ_j	$\Psi_{j.max\,load}$	Energy dissipated (kN.m.rad)
	$M_{j.Rd}$	$M_{j.max}$	$M_{\theta Cd}$	$S_{j.ini}$	$S_{j.p-l}$	$S_{j.ini}/S_{j.p-l}$	$\theta_{M.Rd}$	$\theta_{min.K.R}$	$\theta_{Msup.k.R}$	$\theta_{Mj.max}$	θ_{Cd}			
1--1	1.78	1.60	1.61	1.51	5.00	0.30	0.52	1.26	0.50	0.44	0.44	0.84	0.84	0.71
2--2	1.80	1.25	1.27	0.38	2.28	0.17	2.17	2.79	0.61	0.35	0.35	0.16	0.16	0.45
3--3	3.14	3.78	3.64	0.63	4.12	0.15	0.88	3.22	0.57	0.36	0.36	0.41	0.41	1.32
7--7	2.05	2.24	2.24	0.37	7.00	0.06	0.70	2.09	0.25	0.24	0.24	0.25	0.25	0.41
8--8	1.20	2.27	2.27	0.37	11.00	0.04	0.47	1.43	0.16	0.24	0.24	0.51	0.51	0.54
9--9	4.08	2.69	2.72	0.60	1.88	0.31	1.91	5.81	0.53	0.40	0.39	0.20	0.20	1.07
13--13	1.53	1.49	1.53	0.60	3.36	0.18	0.48	2.44	0.22	0.15	0.14	0.28	0.30	0.21
14--14	3.36	2.14	2.14	0.42	3.48	0.12	1.49	5.00	0.31	0.24	0.23	0.15	0.16	0.49

T300 types double row bolt connections (B240-T300-H_{max}-X_{max}-2-14-L60 (1), B240-T300-H_{min}-X_{max}-2-14-L60 (2) and B240-T300-H_{mid}-X_{max}-2-14-L60 (3)) average experiment and numerical analysis results were compared. As a result of the comparison, a multiplier was created between the experiment results and the numerical results. These values are determined as 2.24 for $M_{j.Rd}$, 2.21 for $M_{j.max}$, 2.18 for $M_{\theta Cd}$, 0.21 for $S_{j.ini}/S_{j.p-l}$, 1.19 for $\theta_{M.Rd}$ and 0.38 for $\theta_{Mj.max}$ and θ_{Cd}. For Ψ_j and $\Psi j.max\,load$ value is rate 0.47. For Energy Dissipated is rate 0.82.

T270 types double row bolt connections (B240-T270-H_{max}-X_{max}-2-14-L60 (7), B240-T270-H_{min}-X_{max}-2-14-L60 (8) and B240-T270-H_{mid}-X_{max}-2 -14-L60 (9)) average experiment and numerical analysis results were compared. For $M_{j.Rd}$ value, numerical analysis results are obtained by multiplying the experiment results by 2.44. For $M_{j.max}$ value rate is 2.41. For $S_{j.ini}/S_{j.p-l}$, this value was calculated as 0.13. The numerical analysis value of $\theta_{M.Rd}$ is obtained by multiplying the experiment result by 1.03. The experiment $\theta_{Mj.max}$ and θ_{Cd} value is multiplied by 0.29 to obtain the numerical analysis. Numerical analysis results can be found by multiplying the experimental Ψ_j and $\Psi_{j.max\,load}$ values by 0.32. For Energy Dissipated is rate 0.67.

T240 type single row bolted connections (B240-T240-H_{max}-X_{max}-2-14-L60 (13) and B240-T240-H_{min}-X_{max}-2-14-L60 (14)) average experiment and numerical analysis results were compared. When the experiment A value is multiplied by 2.45, the result of numerical analysis is obtained. It happened when $M_{j.max}$ was multiplied by 1.82. At $M_{\theta Cd}$, numerical analysis results were 1.84 times the experiment results. In $S_{j.ini}/S_{j.p-l}$, this value was calculated as 0.15. Considering the $\theta_{Mj.max}$ and θ_{Cd} values, the ratio between experiment and numerical results is 0.19. When we look at the experimental Ψ_j and numerical Ψ_j ratios, this value was found to be 0.22. When the experiment $\Psi_{j.max\,load}$ value is multiplied by 0.22, the result of numerical analysis is obtained. Energy Dissipated; experiment results are multiplied by 0.35 and numerical analysis results are obtained.

3.2. T300, T270, T240 types single row bolted connection series.

Fig. 10 shows the moment-rotation curves of the T300, T270, and T240 angle groups. Fig. 11 shows the experiment models. Table 8 summarizes the experiment results. Comparison of experiment results of angle group combinations is shown in Table 9.

Moment-strain graphics of the experiments are shown in Fig. 12.

The values obtained from the strain gauges placed at the 1, 2, 3 and 4 points of the samples are shown in Fig. 12. Since the value could not be obtained at 4 points of the B240-T300-H_{min}-X_{min}-1-14-L60 sample, it is not presented in the graph.

Table 10 shows that comparison of T300, T270, T240 single row bolted connections according to H_{max}, H_{min}, H_{mid} states.

Table 8. Test results of T300, T270, T240 single row bolt combinations.

Experiment	Resistance (kN.m)				Stiffness (kN.m/rad)			Rotation (rad)					Ψ_j	$\Psi_{j.max\,load}$	Energy dissipated (kN.m.rad)
	KR (knee-range)	$M_{j.Rd}$	$M_{j.max}$	$M_{\theta Cd}$	$S_{j.ini}$	$S_{j.p-l}$	$S_{j.ini}/S_{j.p-l}$	$\theta_{M.Rd}$	$\theta_{min.KR}$	$\theta_{Msup.k.R}$	$\theta_{Mj.max}$	θ_{Cd}			
B240-T300-H_{max}-X_{min}-1-14 —L60 (4)	2.36-10.53	10.17	13.57	13.45	0.53	0.35	1.49	0.057	0.016	0.059	0.081	0.081	1.42	1.42	0.54
B240-T300-H_{min}-X_{min}-1-14-L60 (5)	3.47-15.08	8.80	16.63	16.63	3.18	0.26	12.33	0.0064	0.0028	0.054	0.066	0.066	10.31	10.31	0.55
B240-T300-H_{mid}-X_{min}-1-14 —L60 (6)	0.94-11.25	8.37	16.82	16.82	0.58	0.44	1.31	0.042	0.005	0.057	0.092	0.092	2.19	2.19	0.77
B240-T270-H_{max}-X_{min}-1-14-L60 (10)	5.48-6.71	5.48	15.67	15.67	6.1	0.37	16.48	0.021	0.0021	0.015	0.095	0.095	4.23	4.23	0.74
B240-T270-H_{min}-X_{min}-1-14-L60 (11)	2.64-8.98	2.99	14.58	14.58	0.89	0.49	1.78	0.014	0.011	0.056	0.101	0.101	7.21	7.21	1.47
B240-T270-H_{mid}-X_{min}-1-14-L60 (12)	2.76-8.32	3.82	15.67	14.91	0.25	0.71	0.35	0.034	0.028	0.051	0.078	0.079	2.32	2.29	0.59
B240-T240-H_{max}-X_{min}-1-14-L60 (16)	2.60-13.67	8.39	16.86	16.66	0.75	0.44	1.70	0.058	0.02	0.11	0.156	0.156	2.68	2.58	1.29
B240-T240-H_{min}-X_{min}-1-14-L60 (17)	4.66-12.95	11.72	13.39	13.31	1.40	0.071	19.44	0.019	0.0077	0.056	0.063	0.063	3.36	3.36	0.42
B240-T240-H_{mid}-X_{min}-1-14-L60 (18)	9.00-16.051	9.00	16.80	16.41	1.68	0.41	4.11	0.027	0.027	0.068	0.078	0.079	2.92	2.88	0.65

Table 9. T300, T270, T240 Comparison of test results of single row bolted joints (own groups).

Exp.	Resistance (kN.m)			Stiffness (kN.m/rad)			Rotation (rad)					Ψ_j	$\Psi_{j.max\,load}$	Energy dissipated (kN.m.rad)
	$M_{j.Rd}$	$M_{j.max}$	$M_{\theta Cd}$	$S_{j.ini}$	$S_{j.p-1}$	$S_{j.ini}/S_{j.p-1}$	$\theta_{M.Rd}$	$\theta_{min.KR}$	$\theta_{Msup.k.R}$	$\theta_{Mj.max}$	θ_{Cd}			
4—5	13.471	-22.550	-23.643	-500.000	25.714	-727.517	88.772	82.500	8.475	18.519	18.519	-626.056	-626.056	-1.852
4—6	17.699	-23.950	-25.056	-9.434	-25.714	12.081	26.316	68.750	3.390	-13.580	-13.580	-54.225	-54.225	-42.593
5—6	4.886	-1.143	-1.143	81.761	-69.231	89.376	-556.250	-78.571	-5.556	-39.394	-39.394	78.758	78.758	-40.000
10—11	45.438	6.956	6.956	85.410	-32.432	89.199	-566.667	-423.810	-273.333	-6.316	-6.316	84.059	84.059	-98.649
10—12	30.292	0.000	4.850	95.902	-91.892	97.876	-1519.048	-1233.333	-240.000	17.895	16.842	94.871	94.937	20.270
11—12	-27.759	-7.476	-2.263	71.910	-44.898	80.337	-142.857	-154.545	8.929	22.772	21.782	67.822	68.239	59.864
16—17	-39.690	20.581	20.108	-86.667	83.864	-1043.529	67.241	61.500	49.091	59.615	59.615	-25.373	-30.233	67.442
16—18	-7.271	0.356	1.501	-124.000	6.818	-141.765	53.448	-35.000	38.182	50.000	49.359	-8.955	-11.628	49.612
17—18	23.208	-25.467	-23.291	-20.000	-477.465	78.858	-42.105	-250.649	-21.429	-23.810	-25.397	13.095	14.286	-54.762
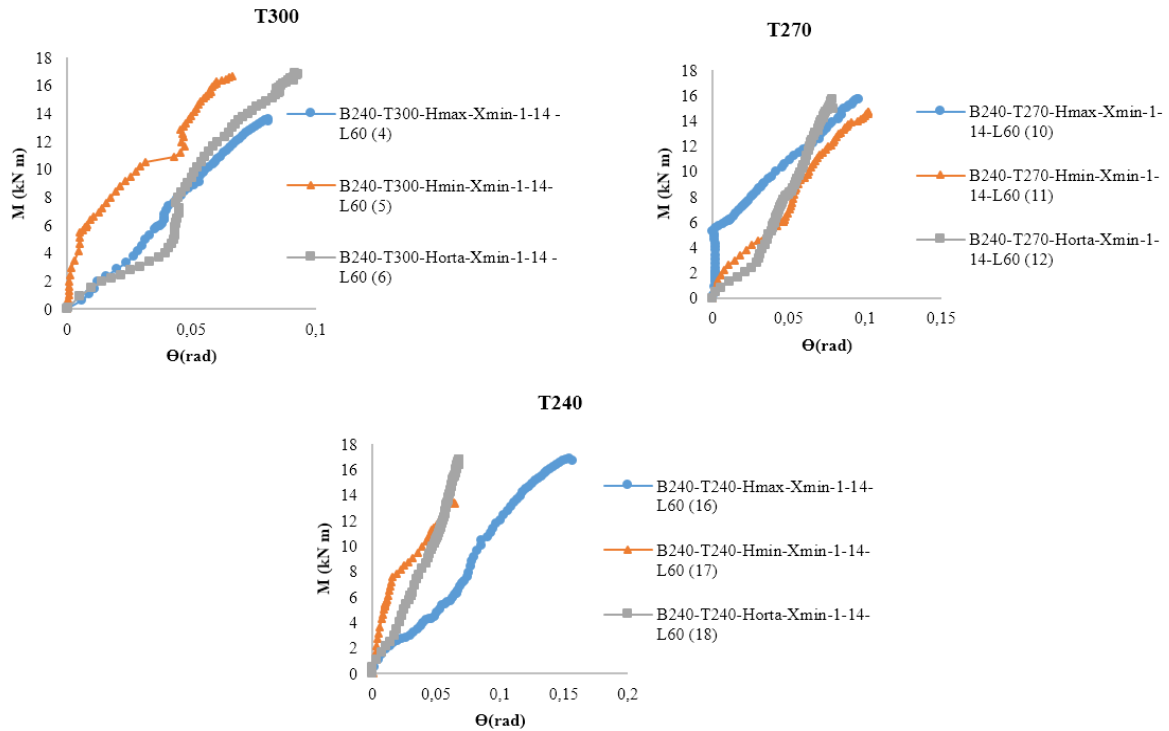
Fig. 10. T300-270-240 group moment-rotation curves of single row bolt tests.

Fig. 11. Experimental models.

B240-T300-Hmin-Xmin-1-14-L60 (5)

B240-T270-Hmin-Xmin-1-14-L60 (11)

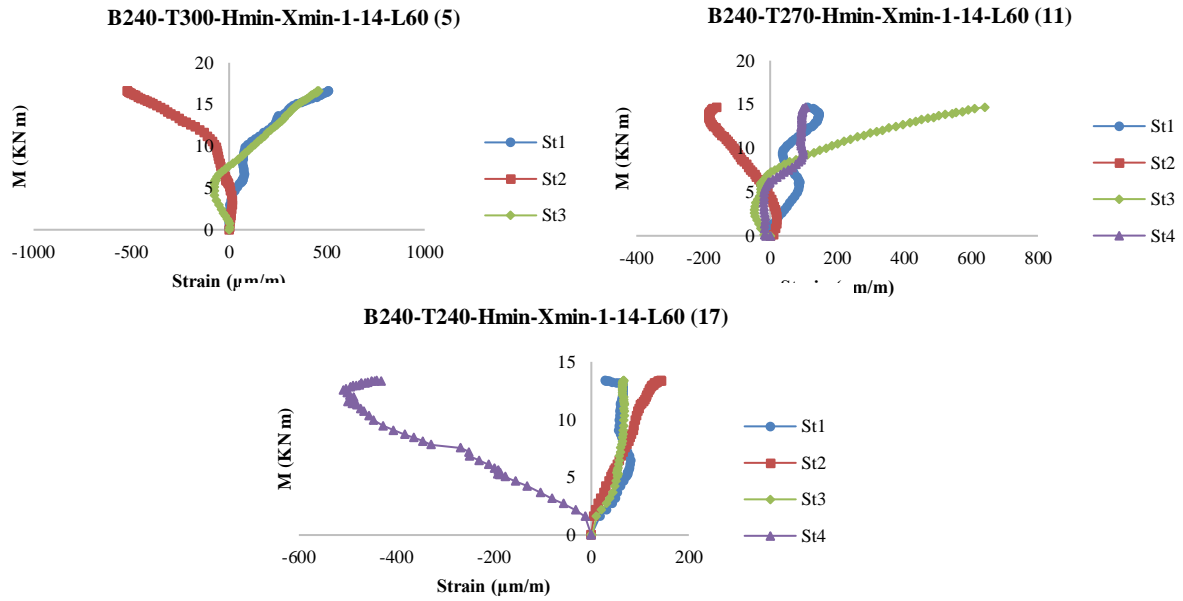**B240-T240-Hmin-Xmin-1-14-L60 (17)**

Fig. 12. Moment–strain curves for T300-T270 and T240 type single row bolts.

Table 10. T300, T270, T240 comparison of single row bolted joints according to H_{max}, H_{min}, H_{mid} states.

Exp.	Resistance (kN.m)			Stiffness (kN.m/rad)			Rotation (rad)					Ψ_j	$\Psi_{j.max\ load}$	Energy dissipated (kN.m.rad)
	$M_{j.Rd}$	$M_{j.max}$	$M_{\theta Cd}$	$S_{j.ini}$	$S_{j.p-1}$	$S_{j.ini}/S_{j.p-1}$	$\theta_{M.Rd}$	$\theta_{min.K.R}$	$\theta_{Msup.k.R}$	$\theta_{Mj.max}$	θ_{Cd}			
4--10	46.116	-15.475	-16.506	-1050.943	-5.714	-1006.040	96.316	86.875	74.576	-17.284	-17.284	-3085.21	-3085.211	-37.037
4--16	17.502	-24.245	-23.866	-41.509	-25.714	-14.094	-1.754	-25.000	-86.441	-92.593	-92.593	-88.732	-81.690	-138.889
10--16	-53.102	-7.594	-6.318	87.705	-18.919	89.684	-2661.905	-852.381	-633.333	-64.211	-64.211	94.075	94.296	-74.324
5--11	66.023	12.327	12.327	72.013	-88.462	85.564	-118.750	-292.857	-3.704	-53.030	-53.030	30.068	30.068	-167.273
5--17	-33.182	19.483	19.964	55.975	72.692	-57.664	-196.875	-175.000	-3.704	4.545	4.545	67.410	67.410	23.636
11--17	-291.973	8.162	8.711	-57.303	85.510	-992.135	-35.714	30.000	0.000	37.624	37.624	53.398	53.398	71.429
6--12	54.361	6.837	11.356	56.897	-61.364	73.282	19.048	-460.000	10.526	15.217	14.130	-5.936	-4.566	23.377
6--18	-7.527	0.119	2.438	-189.655	6.818	-213.740	35.714	-440.000	-19.298	15.217	14.130	-33.333	-31.507	15.584
12--18	-135.602	-7.211	-10.060	-572.000	42.254	-1074.286	20.588	3.571	-33.333	0.000	0.000	-25.862	-25.764	-10.169

3.2.1. Failure mechanism

According to Eurocode 3, three types of breaking performance have been proposed for face plate joints. The first kind of breakage is that there is only deformation in the plate (Fig. 13a). The second kind of break-

age is deformation and bolt breakage (show that Fig. 13b), and the third type is just bolt breakage (Fig. 13c). As seen in Fig. 13, this kind of cutting and breaking is the first kind of breaking situation. In other words, in the proposed combination, the first kind of breakage occurs.

B240-T300-H_{min}-X_{min}-1-14-L60 (5)

B240-T270-H_{min}-X_{min}-1-14-L60 (11)

B240-T240-H_{min}-X_{min}-1-14-L60 (17)

Fig. 13. Collapse models.

Looking at $M_{j.Rd}$ values; T300 largest value in the group appears to be in H_{max}-X_{min} group. Referring to these values in the group appears to be in the H_{min}-X_{min} group T270. With the increase of H value, BB value increased in all groups. The highest change was seen in the T270 group when the H_{max}-X_{min} and H_{min}-X_{min} groups were compared, an increase of 45.43%.

3.2.2. Finite element models

Fig. 14 shows the moment-rotation curves obtained by the finite element's model. The results obtained from the curves are given in Table 11. Comparison of finite elements with experiment results is given in Table 12.
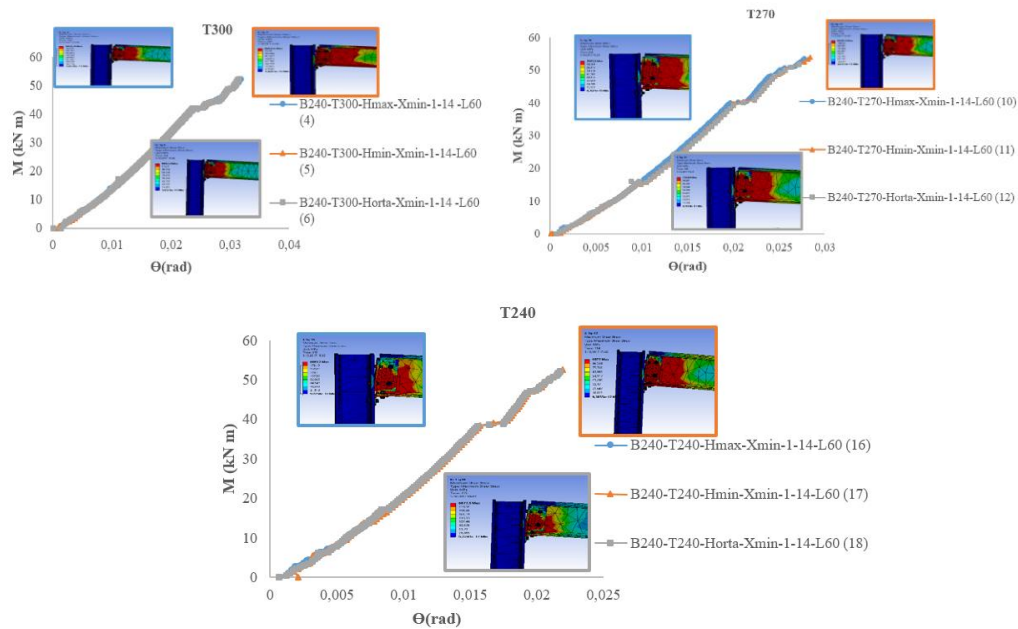

Fig. 14. T300, T270 and T240 group moment-rotation curves of single row bolt finite element models.

Table 11. T300, T270, T240 type single row bolt finite element model experiment results.

Experiment	Resistance (kN.m)			Stiffness (kN.m/rad)			Rotation (rad)					Ψ_j	$\Psi_{j.max\,load}$	Energy dissipated (kN.m.rad)
	KR (knee-range)	$M_{j.Rd}$	$M_{j.max}$	$M_{\theta Cd}$	$S_{j.ini}$	$S_{j.p-1}$	$S_{j.ini}/S_{j.p-1}$	$\theta_{M.Rd}$	$\theta_{min.K.R}$	$\theta_{Msup.k.R}$	$\theta_{Mj.max}$	θ_{Cd}			
B240-T300-H_{max}-X_{min}-1-14 -L60 (4)	41.75-48.64	42.79	52.08	52.08	1.05	0.61	1.721	0.025	0.023	0.029	0.032	0.032	1.280	1.280	0.8333
B240-T300-H_{min}-X_{min}-1-14-L60 (5)	41.75-48.64	42.79	51.03	51.03	1.05	0.61	1.721	0.025	0.023	0.029	0.031	0.031	1.240	1.240	0.7910
B240-T300-H_{mid}-X_{min}-1-14 -L60 (6)	41.75-48.69	42.79	52.09	52.09	1.05	0.61	1.721	0.025	0.023	0.029	0.031	0.031	1.240	1.240	0.8074
B240-T270-H_{max}-X_{min}-1-14-L60 (10)	39.15-40.05	43.65	53.57	53.57	0.93	0.51	1.824	0.021	0.02	0.021	0.027	0.027	1.286	1.286	0.7232
B240-T270-H_{min}-X_{min}-1-14-L60 (11)	39.15-42.75	40.95	54.00	54.00	0.85	0.70	1.214	0.021	0.02	0.022	0.028	0.028	1.333	1.333	0.7560
B240-T270-H_{mid}-X_{min}-1-14-L60 (12)	39.15-42.75	40.95	51.75	51.75	0.85	0.70	1.214	0.021	0.02	0.022	0.027	0.027	1.286	1.286	0.6986
B240-T240-H_{max}-X_{min}-1-14-L60 (16)	38.18-45.02	41.40	52.53	52.23	0.94	0.073	12.877	0.017	0.016	0.019	0.022	0.022	1.294	1.294	0.5745
B240-T240-H_{min}-X_{min}-1-14-L60 (17)	38.18-45.02	41.40	52.53	52.23	0.94	0.073	12.877	0.017	0.016	0.019	0.022	0.022	1.294	1.294	0.5745
B240-T240-H_{mid}-X_{min}-1-14-L60 (18)	38.18-45.02	41.46	52.56	52.26	0.94	0.073	12.877	0.017	0.016	0.019	0.022	0.022	1.294	1.294	0.5749

Table 12. T300, T270, T240 type single row bolt finite element model and comparison of experimental results.

Exp.	Resistance (kN.m)			Stiffness (kN.m/rad)			Rotation (rad)					Ψ_j	$\Psi_{j.max\,load}$	Energy dissipated (kN.m.rad)
	$M_{j.Rd}$	$M_{j.max}$	$M_{\theta Cd}$	$S_{j.ini}$	$S_{j.p-1}$	$S_{j.ini}/S_{j.p-1}$	$\theta_{M.Rd}$	$\theta_{min.K.R}$	$\theta_{Msup.k.R}$	$\theta_{Mj.max}$	θ_{Cd}			
4--4	4.21	3.84	3.87	1.98	1.74	1.16	0.44	1.44	0.49	0.40	0.40	0.90	0.90	1.54
5--5	4.86	3.07	3.07	0.33	2.35	0.14	3.91	8.21	0.54	0.47	0.47	0.12	0.12	1.44
6--6	5.11	3.10	3.10	1.81	1.39	1.31	0.60	4.60	0.51	0.34	0.34	0.57	0.57	1.05
10--10	7.97	3.42	3.42	0.15	1.38	0.11	10.00	9.52	1.40	0.28	0.28	0.03	0.03	0.98
11--11	13.70	3.70	3.70	0.96	1.43	0.68	1.50	1.82	0.39	0.28	0.28	0.18	0.18	0.51
12--12	10.72	3.30	3.47	3.40	0.99	3.47	0.62	0.71	0.43	0.35	0.34	0.55	0.56	1.18
16--16	4.93	3.12	3.14	1.25	0.17	7.57	0.29	0.80	0.17	0.14	0.14	0.48	0.50	0.45
17--17	3.53	3.92	3.92	0.67	1.03	0.66	0.89	2.08	0.34	0.35	0.35	0.39	0.39	1.37
18--18	4.61	3.13	3.18	0.56	0.18	3.13	0.63	0.59	0.28	0.28	0.28	0.44	0.45	0.88

4. Conclusions

Looking at the $M_{j.Rd}$ values; T300 largest value in the group appears to be in H_{max}-X_{min} group. Referring to these values in the group appears to be in the H_{min}-X_{min} group T270. With the increase of H value, BB value increased in all groups. The highest change was seen in the T270 group when the H_{max}-X_{min} and H_{min}-X_{min} groups were compared, an increase of 45.43%.

Considering A and B values; it is seen that the largest value of the T300 group is in the H_{mid}-X_{min} group. Looking at these values for the T270 and T240 groups, it is seen that they are in the H_{max}-X_{min} and H_{mid}-X_{min} groups. But the T240 in the combination group and H_{max}-X_{max} and H_{mid}-X_{max} group have the highest. When all groups with an increase in the H value has increased the value of $M_{\theta Cd}$ and $M_{j.max}$. It is seen that H_{mid} values are higher than H_{min} values in T300 and T270 groups. The thickness of the combination should be selected types of joint's increases H_{mid}. $M_{\theta Cd}$, the highest increases in the T240 group H_{max}-X_{min} and H_{min}-X_{min} group has been increased by %20.10. Likewise, this ratio is %20.58 in $M_{j.max}$.

T connection elements through the wall thickness increase stiffness reduction is observed. Data were seen to be the largest in the value H_{min} examined. So are the rigid connections. H_{max} or H_{mid} should be used to reduce stiffness.

References

Abdalla KM, Chen WF (1995). Expanded database of semi-rigid steel connections. *Computers & Structures*, 56(4), 553-564.

Aydın AC, Kılıç M, Maali M, Sağıroğlu M (2015a). Experimental assessment of the semi-rigid connections behavior with angles and stiffeners. *Journal of Constructional Steel Research,* 114, 338-348.

Aydın AC, Kılıç M, Maali M, Sağıroğlu M (2015b). Experimental investigation of sinus beams with end-plate connections. *Thin-Walled Structures*, 97, 35-43.

Batho C, Rowan H (1934). Investigations on beam and stanchion connections. *Second Report of the Steel Structures Research Committee*, London.

Coelho AMG, Bijlaard FS (2007). Experimental behaviour of high strength steel end-plate connections. *Journal of Constructional Steel Research*, 63(9), 1228-1240.

Díaz C, Victoria M, Martí P, Querin OM (2011). FE model of beam-to-column extended end-plate joints. *Journal of Constructional Steel Research*, 67(10), 1578-1590.

Kukreti AR, Zhou FF (2006). Eight-bolt endplate connection and its influence on frame behavior. *Engineering Structures*, 28(11), 1483-1493.

Maali M, Kılıç M, Aydın AC (2016). Experimental model of the behaviour of bolted angles connections with stiffeners. *International Journal of Steel Structures*, 16(3), 719-733.

Maali M, Kılıç M, Sağıroğlu M, Aydın AC (2017). Experimental model for predicting the semi-rigid connections' behaviour with angles and stiffeners. *Advances in Structural Engineering*, 20(6), 884-895.

Maali M, Aydın AC, Showkati H, Sağıroğlu M, Kılıç M (2018a). The effect of longitudinal imperfections on thin-walled conical shells. *Journal of Building Engineering*, 20, 424-441.

Maali M, Sagiroglu M, Solak MS (2018b). Experimental behavior of screwed beam-to-column connections in cold-formed steel frames. *Arabian Journal of Geosciences*, 11(9), 1-6.

Piluso V, Rizzano G (2008). Experimental analysis and modelling of bolted T-stubs under cyclic loads. *Journal of Constructional Steel Research*, 64(6), 655-669.

Shi G, Shi Y, Wang Y, Bradford MA (2008). Numerical simulation of steel pretensioned bolted end-plate connections of different types and details. *Engineering Structures*, 30(10), 2677-2686.

Tagawa H, Gurel S (2005). Application of steel channels as stiffeners in bolted moment connections. *Journal of Constructional Steel Research*, 61(12), 1650-1671.

Tagawa H, Liu Y (2014). Stiffening of bolted end-plate connections with steel member assemblies. *Journal of Constructional Steel Research*, 103, 190-199.

Tagawa H, Nagoya Y, Chen X (2020). Bolted beam-to-column connection with buckling-restrained round steel bar dampers. *Journal of Constructional Steel Research*, 169, 106036.